



Original Research article

Thermostable Polarizing Film on the Basis of Poly (vinyl alcohol) and New Dichroic Synthesized Azo Dye for Optical Applications: Theoretical and Experimental Investigations

Siyamak Shahab^{1,2} * , Liudmila Filippovich^{1,2} , Masoome Sheikhi³*

¹Institute of Physical Organic Chemistry, National Academy of Sciences of Belarus, 13 Surganov Str., Minsk 220072, Belarus

²Institute of Chemistry of New Materials, National Academy of Sciences of Belarus, 36 Skarina Str., Minsk 220141, Belarus

³Young Researchers and Elite Club, Gorgan Branch, Islamic Azad University, Gorgan, Iran

ARTICLE INFO

Article history

Submitted: 2023-06-13

Revised: 2023-08-29

Accepted: 2023-08-30

Manuscript ID: CHEMM-1708-1009

Checked for Plagiarism: Yes

Language Editor:

Ermia Aghaie

Editor who approved publication:

Dr. Mohammad A. Khalilzadeh

DOI: 10.48309/chemm.2023.53193

KEYWORDS

Thermostable polarizing PVA-film

DFT calculation

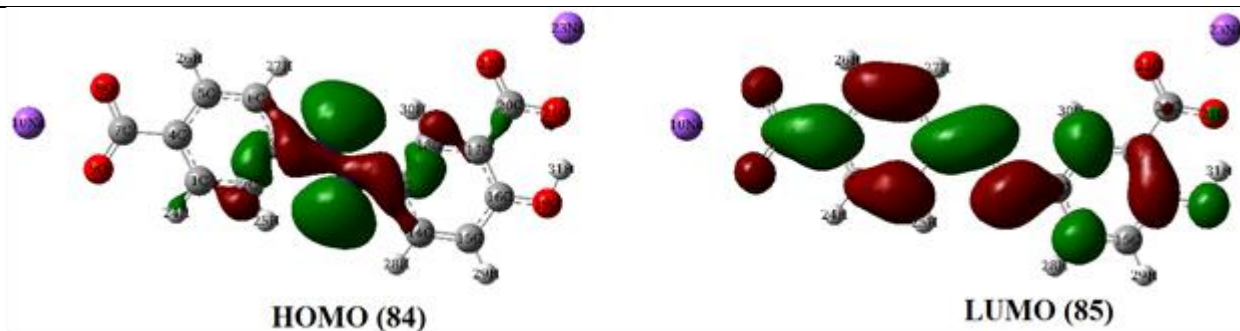
Thermal conductivity

UV-Vis spectrum

ABSTRACT

Quantum-chemical calculations using the Density Functional Theory (DFT) approach for structural analysis of the new dichroic mono azo dye: Sodium (*E*)-5-((4-carboxylatophenyl)diazenyl)-2-hydroxybenzoate (**S**) (trans isomer) was carried out using B3LYP methods with 6-311+G* basis set. After calculations, the new mono azo dye was synthesized. UV, FT-IR and ¹H NMR spectra of the compound **S** are reported. The electronic spectrum of the mono azo dye **S** was also carried out in the water solution. Interpretation of absorption strips in UV region of spectrum was also reported. On the basis of the polyvinyl alcohol (PVA) and the new dichroic synthesized azo dye thermostable polarizer film absorbing in the UV region of spectrum ($\lambda_{\max}=388$ nm) with effect of polarization (PE) in the absorption maximum 97% was developed. The main spectral-polarization parameters (transmittance, optical density) of stretched PVA-films were measured and discussed. It was also established that oriented colored PVA-films is phenomenon of anisotropy of thermal conductivity ($\lambda_{\parallel} / \lambda_{\perp}$). Thermal conductivity in the direction of orientation (λ_{\parallel}) is higher than in the direction perpendicular to the orientations (λ_{\perp}). The developed thermostable polarizer film was used in polarizing microscopes, circular polarizers, magnetometers, spectropolarimeters and electrical signals sensors.

GRAPHICAL ABSTRACT



* Corresponding author: Siyamak Shahab

E-mail: siyamak.shahab@yahoo.com & m.sheikhi2@gmail.com

© 2023 by SPC (Sami Publishing Company)

Introduction

PVA-Polarizing thin polymer films are widely used in various fields [1-8]. There are various types of thin -PVA-polarizers, but the ones that are mostly used in the practice are obtained on the basis of PVA, colored by iodine or organic dyes such as stilbene and anthraquinone derivatives and especially with azo compounds, which are more resistant to high temperatures and humidity of the environment in comparison with iodine polarizer, but inferior to them in the spectral and polarization characteristics [6-10]. In addition, recent development in nanotechnology showed that anisotropic inorganic nanoparticles could be used as dichroic components of polarizing films, increasing the stability of polarizers in high-moisture and high-temperature environments. Currently, in variety of electronic and optical devices used in industrial, special and household polarizers are required, not only improving the contrast, brightness and stability of the indicators, but also working in a wide spectral range including UV, visible, and near IR regions of spectrum [11]. However, such polarizers with high polarization efficiency in a wide spectral range and with the necessary light stability to UV irradiation practically not developed. Obviously, the research aimed at the creation of domestic polarizing film operating in the UV, visible and near IR regions of the spectrum with high polarizing efficiency and increased light stability are required [8-13].

The aim of this work was to develop the thermostable polarizer film on the basis of PVA and the new synthesized dichroic azo component absorbing in UV region of the spectrum with the polarizing efficiency 97%.

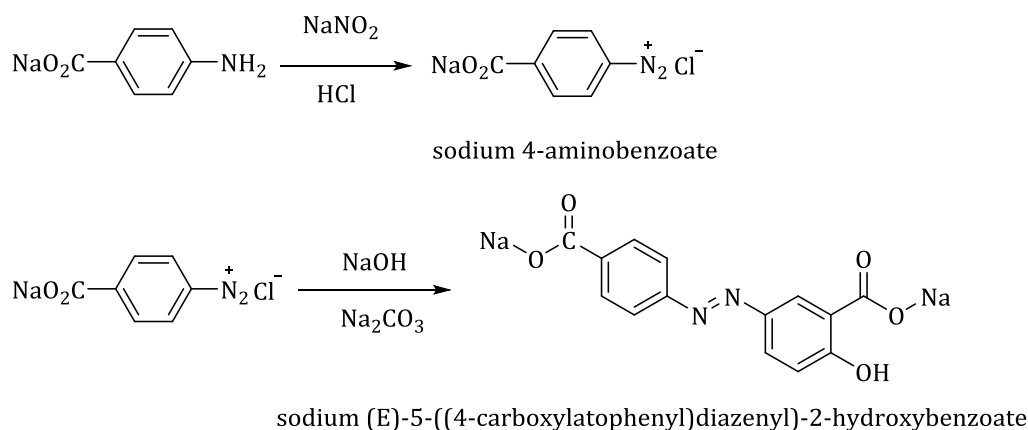
Experimental

Reagent and apparatus

All chemicals and apparatus were presented in our work [1].

Synthesis of Sodium (*E*)-5-((4-carboxylatophenyl)diazenyl)-2-hydroxybenzoate (*S*)

14 g of sodium 4-aminobenzoate was grinded in a mortar with 210 ml of water and 51.6 g of concentrated hydrochloric acid and diazotized with 40 ml of 35% strength sodium nitrite. After the addition of sodium nitrite, it was stirred for 10 min at 2 °C. The resulting diazo solution was poured into a solution consisting of 25 g of salicylic acid in 150 ml of water and 40 g Na₂CO₃. The resulting mixture was allowed to stand overnight in the refrigerator. If azo coupling is not completely gone, add a 25% NaOH. The resulting paste is filtered and the precipitate was recrystallized from a minimum amount of water. The disodium salt of (*E*)-5-((4-carboxyphenyl)diazenyl)-2-hydroxybenzoic acid as a dark brown amorphous powder (Scheme 1).



Scheme 1: Preparation of Sodium (*E*)-5-((4-carboxylatophenyl)diazenyl)-2-hydroxybenzoate (*S*)

Experimental and calculated IR spectrum of the compound S is presented in Table 1. The Most significant calculated and experimental vibrational modes are summarized in Table 1. The theoretical IR spectrum of optimized molecule was calculated using the DFT/B3LYP/6-311+G* method. Density functional theory at the B3LYP/6-311+G* level reproduce IR

spectral data reasonably accurately when a uniform scaling factor of 0.98 over the complete spectral range is employed. The synthesized compound has the main vibration modes at 833 (γ_{C-H} , δ_{ring}) cm^{-1} , 1211, 1229 (ν_{C-C} , ν_{C-N} , β_{C-H}) cm^{-1} , 1461, 1485 (ν_{asC-C} , $\nu_{N=N}$, β_{C-H} , $\nu_{C=O}$) cm^{-1} , 1632 ($\tau_{C=O}$, β_{C-C}) cm^{-1} , 3442 (ν_{O-H} , ν_{C-H}) cm^{-1} .

Table 1: The Main Vibrational Frequencies and Their Assignment of the compound S

ν_{exp}, cm^{-1}	ν_{calc}, cm^{-1}	Vibrational assignment
3442vw	3638	ν_{O-H}, ν_{C-H}
	3260	ν_{C-H}
	3253	ν_{C-H}
	3247	ν_{C-H}, ν_{asC-H}
	3244	ν_{C-H}
	3233	ν_{C-H}, ν_{asC-H}
2821vw	3183	ν_{C-H}
	1661	β_{C-C}
1632vw	1640	$\tau_{C=O}, \beta_{C-C}$
	1546	ν_{asC-C}
1588s	1587	ν_{ring}
1461vw,1485vw	1475	$\nu_{asC-C}, \nu_{N=N}, \beta_{C-H}, \nu_{C=O}$
1444w	1446	ν_{asC-C}, β_{C-H}
	1430	β_{C-H}
	1420	$\beta_{C=O}, \beta_{C-C}$
	1388	ν_{sC-C}, β_{C-H}
	1385w	1384
1339m	1343	β_{C-C}
	1328	ν_{asC-C}, β_{C-H}
	1298	β_{C-H}
1301vw	1268	ν_{C-C}, ν_{C-N}
	1223	$\nu_{C-C}, \nu_{C-N}, \beta_{C-H}$
1229vw	1223	$\nu_{C-C}, \nu_{C-N}, \beta_{C-H}$
1211vw	1203	$\nu_{C-C}, \nu_{C-N}, \beta_{C-H}$
1194m	1189	ν_{C-C}, β_{C-H}
1174m	1172	β_{C-H}
	1144	β_{C-H}
1101m	1096	$\gamma_{C-H}, \beta_{C-H}$
1070m	1090	β_{C-H}
	1049	β_{C-H}
1039m	1043	δ_{ring}
1008m	1014	$\gamma_{C-H}, \tau_{ring}$
	995	τ_{ring}
833vw	960	γ_{C-H}
	936	γ_{C-H}
	916	γ_{C-H}
	847	γ_{C-H}
	839	$\gamma_{C-H}, \delta_{ring}$
	815	β_{C-C}
811vw	822	τ_{ring}
	805	$\gamma_{C-H}, \tau_{ring}, \delta_{ring}, \delta_{O-H}$

	750	β_{C-H}
	759	τ_{ring}
	726	$\gamma_{C-H}, \tau_{ring}$
	722	$\gamma_{C-H}, \tau_{ring}$
684s	686	$\gamma_{C-H}, \tau_{ring}$
636s	655	τ_{ring}
	602	τ_{ring}
589s	589	τ_{ring}
	570	β_{ring}
	539	γ_{C-H}
	521	β_{ring}
	489	$\beta_{C=O}, \beta_{C-H}$
	482	$\gamma_{ring}, \tau_{O-H}$
	437	ω_{ring}
	436	ω_{ring}
	434	τ_{ring}
	431	$\gamma_{ring}, \omega_{O-H}$
	426	β_{C-H}, β_{C-C}
	400	ω_{ring}
	391	ω_{ring}
	366	β_{C-N}
	334	γ_{C-N}
	288	τ_{ring}
	270	τ_{ring}
	262	$\beta_{C=O}$
	250	γ_{C-N}
	221	$\beta_{C=O}, \beta_{C-H}$
	202	γ_{C-N}
	154	β_{C-H}
	145	$\gamma_{C-H}, \gamma_{N=N}$
	144	$\gamma_{C-H}, \gamma_{N=N}$
	118	$\beta_{C=O}, \beta_{C-H}$
	110	γ_{C-H}
	75	γ_{C-H}
	65	γ_{C-H}
	58	γ_{C-H}
	31	γ_{C-H}
	30	γ_{C-H}
	22	γ_{C-H}
	18	γ_{C-H}

τ – torsion, γ – out of plane bending, β – in plane bending, ν – stretching, ν_s – symmetric stretching, ν_{as} – antisymmetric stretching

s – strong, ms – medium strong, m – medium, w – weak, vw – very weak

1H NMR spectral analysis of the title compound was enhanced by the use of 1H NMR spectroscopy. To perform quantum-chemical modeling of 1H NMR spectra, a special algorithm includes the following steps: 1) Transformation of the structural formula to a 3D structure; 2)

Optimization of the geometry of the molecule; 3) Calculation of chemical shifts and 4) Averaging chemical shifts. 1H NMR spectrum of the optimized molecule was also calculated by B3LYP/6-311+G* level of theory. ChemBio Office 2010 software package was used for visualization

of the simulated ^1H NMR spectrum (Figure 1a). Experimental ^1H NMR spectrum of compound is shown in Figure 1b. The theoretical ^1H NMR chemical shifts of the compound S have been compared with the experimental data.

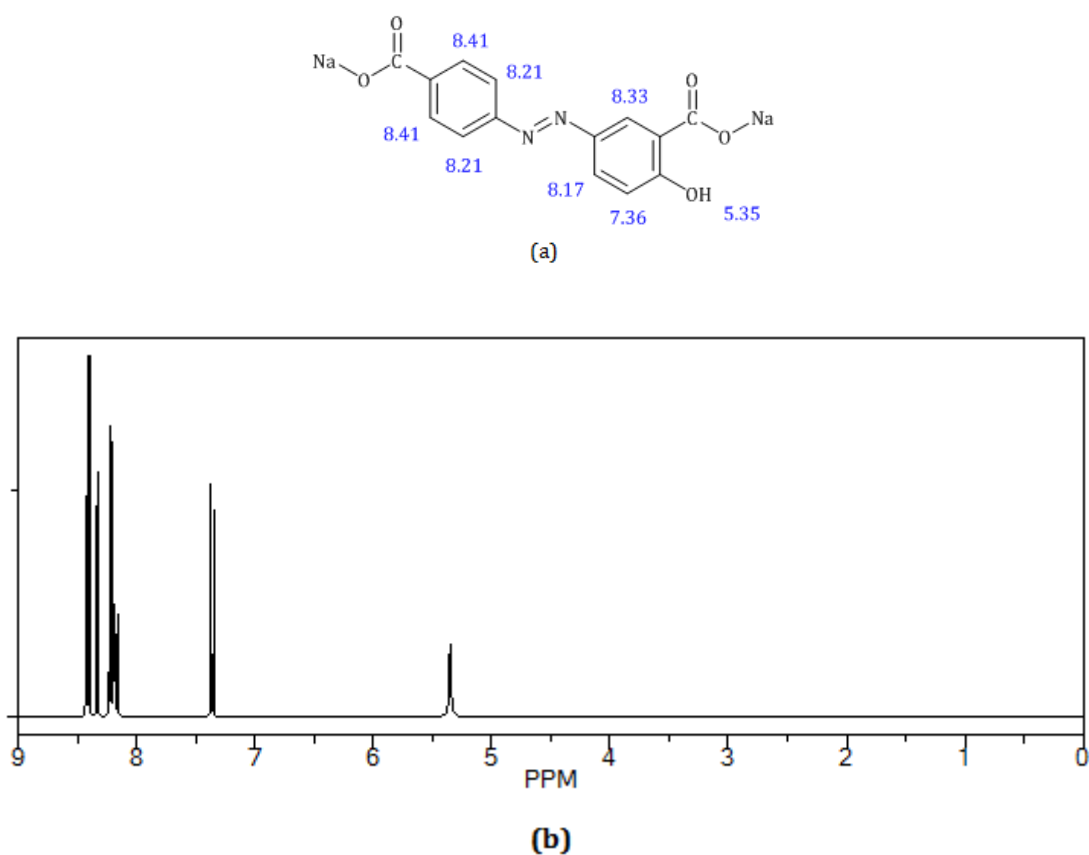


Figure 1: Calculated chemical shifts a) and experimental b) ^1H NMR spectrum of the compound S

The theoretical ^1H NMR spectrum of the molecule was calculated by B3LYP/6-311+G*, B3LYP/6-311+G, B3LYP/6-31+G* and B3LYP/6-31+G** levels of theory that differ from the experimental data (Table 2).

Table 2: The calculated and experimental chemical shifts of the molecule S

Assignments	Calculated shifts				Experimental
	B3LYP/6-311+G*	B3LYP/6-311+G	B3LYP/6-31+G*	B3LYP/6-31+G**	
OH	5.38	5.53	5.54	5.58	5.35
CH	8.39	8.66	8.22	8.64	8.41
CH	8.23	8.33	8.19	8.07	8.21
CH	8.29	8.07	8.51	8.66	8.21
CH	8.47	8.60	8.63	8.58	8.41
CH	8.36	8.60	8.63	8.50	8.33
CH	8.10	8.01	8.04	8.06	8.17
CH	7.39	7.48	8.04	8.06	7.35

According to these results, the calculated chemical shifts calculated by B3LYP/6-311+G* level of theory are in good compliance with the experimental findings. The correlation between experimental and theoretical values proton chemical shifts is 98-99%.

Preparation of PVA-films containing the compound S

The PVA-films were prepared according to our work [1]. The main optical properties of the thin polarizing PVA-films such as Transmittance (T_{max} , T_{min}), polarizing efficiency (PE) and Dichroic Ratio (R_d) were evaluated at the absorption

maximum of the polarizing films according to Equations (1, 2) [1-5, 10]:

$$PE = (T_{max} - T_{min}) / \quad (1)$$

$$(T_{max} + T_{min}) * 100 \quad (2)$$

$$R_d = D_{max} / D_{min}$$

Where, T_{max} , T_{min} , D_{max} and D_{min} - Absorbance and Transmittance for linearly polarized light parallel and perpendicular to direction of stretching of colored film.

Polarizing efficiency of colored oriented PVA-films depends on the concentration of injected dye and Stretching Degree ($R_s = 3.0-4.0$) of the films [12], therefore the optimum concentration of the compound S in PVA-film was obtained (Table 3).

Table 3: The Optical Characteristics of PVA-Films at Different Concentration of the Compound S

[S] in film, wt. %	R_s	Transmittance of films at $\lambda_{max} = 388$ nm, %		Optical Density of films at $\lambda_{max} = 388$ nm, %		PE, %
		T_{max}	T_{min}	D_{max}	D_{min}	
0.05	3	22.1	10.0	1.0	0.7	38
0.05	4	37.6	13.9	0.9	0.4	46
0.10	3	17.2	5.3	1.3	0.8	53
0.10	4	23.5	4.1	1.4	0.6	70
0.18	3	13.2	0.2	2.7	0.9	97
0.18	4	14.2	0.6	2.2	0.9	92
0.20	3	5.7	0.5	2.3	1.2	84
0.20	4	10.9	0.4	2.4	1.0	93

Changes in concentration of the compound S from 0.05 to 0.20 wt.% in the colored oriented PVA-film show that with increasing concentration of the dichroic agent, maximum light transmission in parallel and perpendicular direction are reduced (at same R_s). When $R_s = 3.0$ at [S] = 0.05 wt.% $T_{max} = 22.1\%$, $T_{min} = 10.0\%$. At [S] = 0.10 wt.% $T_{max} = 17.2\%$, $T_{min} = 5.3\%$. At [S] = 0.18 wt.% $T_{max} = 13.2\%$, $T_{min} = 0.2\%$ (photo of the polarizing film containing 0.18 wt.% of the compound S in parallel and perpendicular directions of stretching is presented in Figure 2

a,b). At [S] = 0.20 wt.% $T_{max} = 5.7\%$, $T_{min} = 0.5\%$. When $R_s = 4.0$ at [S] = 0.05 wt.% $T_{max} = 37.6\%$, $T_{min} = 13.9\%$. At [S] = 0.10 wt.% $T_{max} = 23.5\%$, $T_{min} = 4.1\%$. At [S] = 0.18 wt.% $T_{max} = 14.2\%$, $T_{min} = 0.6\%$. At [S] = 0.20 wt.% $T_{max} = 10.9\%$, $T_{min} = 0.4\%$. And when $R_s = 3.0$ at [S] = 0.18 wt.%, PE = 97%. With increasing concentration of the dichroic agent, PE increases. The best optical parameters has PVA-film containing 0.18 wt.% of the compound S ($T_{max} = 13.2\%$, $T_{min} = 0.2\%$, $D_{max} = 2.7\%$, $D_{min} = 0.9\%$ and PE = 97%) at $R_s = 3.0$.

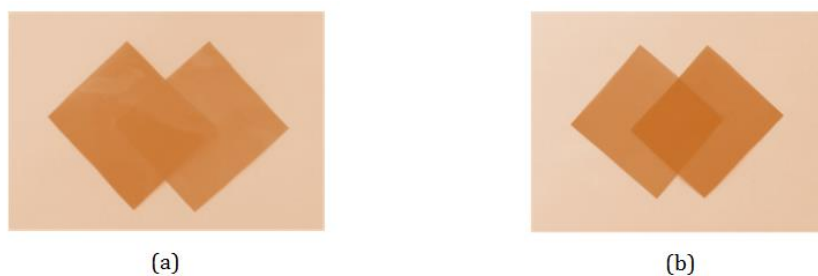


Figure 2: PVA-films containing the 0.18 wt.% of dichroic dye S in parallel (a) and perpendicular (b) directions of stretching

Dichroism (anisotropy of absorption) appears under uniaxial orientation of the colored PVA-films (Figure 3(b)). Dichroic ratio (R_d) of the PVA polarizing film containing 0.18 wt.% of the compound S is (2.7 / 0.9) 3.0.

Anisotropy of thermal conductivity of PVA-films

We have studied thermal conductivity of the systems: PVA-S for development of thermostable

polarizing films according to [5]. The oriented PVA-films with the compound S is the phenomenon of anisotropy of thermal conductivity ($\lambda_{||} / \lambda_{\perp}$) was established. Anisotropy of thermal conductivity in unstretched PVA-films is observed not appreciably as comparison to stretched PVA-films that is observed very clearly (Table 4).

Table 4: Dependence of thermal conductivity on stretching degree in pure PVA-films

R_s	λ , W/m. ^o C		
	$\lambda_{ }$	λ_{\perp}	$\lambda_{ } / \lambda_{\perp}$
1.5	0.876	0.764	1.15
2.0	0.878	0.636	1.38
2.5	0.880	0.549	1.60
3.0	0.881	0.503	1.75
4.0	0.882	0.475	1.86

Results of thermal conductivity measurements of the PVA-films containing the dye S depending on stretching degree are given in Table 5. It is clear from the results that the thermal conductivity in a direction ($\lambda_{||}$) orientation is higher than that of

the perpendicular orientations (λ_{\perp}). On resulting anisotropy at a known degree of extension it is possible to judge anisotropy of chain structure [5].

Table 5: Thermal conductivity of PVA-films containing the dye S at concentration 0.18 wt. %

R_s	λ , W/ m. ^o C		
	$\lambda_{ }$	λ_{\perp}	$\lambda_{ } / \lambda_{\perp}$
2.0	0.876	0.255	3.44
3.0	0.855	0.236	3.62
4.0	0.843	0.174	4.84
5.0	0.836	0.101	8.27

The occurrence of anisotropy of thermal conductivity is connected that at orientation of PVA occurs orientation of the amorphous part of polymer and also formation of additional number of intermolecular connections. Thermal conductivity of PVA films changes after the injection of dye and along an axis of orientation and in perpendicular axis decreases (Table 5).

Computational Details

Structural analysis

The theoretical molecular structure of the new synthesized compound S in the ground state was

optimized by B3LYP/6-311+G* level of theory (Figure 3a). DFT computational calculations were carried out with the Gaussian 09W package [14]. For visualization of UV/Vis spectrum of the compound S GaussView 05 software was used [14]. Geometry optimization in solvent at the ground and excited states was performed. The optimized parameters (bond lengths, angles) of the compound S are presented in Table 6. During optimization process, the compound S was passed through 57 stages to achieve the most stable conformer of the structure (Figure 3a). This conformer has total energy equal -1903.22 Hartree. In order to study interaction between PVA and molecule of the dye S quantum-chemical calculations by B3LYP/6-311+G* level of theory

were carried out (Figure 3b). The dye molecule has two large atoms of sodium (Na(23) and Na(10)). More radii of sodium atoms do not allow the dye molecule and PVA interact. We assume

that the dye molecules mechanically fill the voids between the polymer chains. In this case chemical bond do not arise between them.

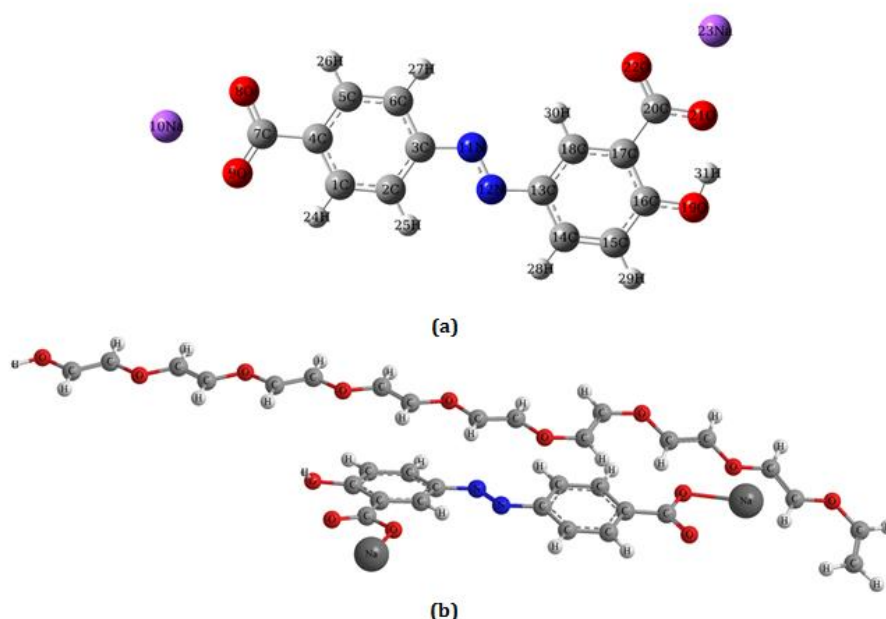


Figure 3: a) Optimized structure of the dichroic dye S; b) Optimized structures of PVA chain (n = 9) and the dichroic dye S

Table 6: The main optimized geometric parameters of the compound S by B3LYP/6-311+G* method

Parameter	Bond length, (Å)	Parameter	Bond Angle (°)
O(22)-Na(23)	2.36	O(21)-K(38)-O(20)	48.05
O(21)-Na(23)	2.34	O(22)-Na(23)-O(21)	56.85
C(20)-O(22)	1.25	Na(23)-O(22)-C(20)	89.94
C(29)-O(21)	1.29	Na(23)-O(21)-C(20)	89.83
O(19)-H(31)	1.02	O(22)-C(20)-C(17)	119.78
C(16)-O(19)	1.34	Na(10)-O(9)-C(7)	88.84
O(8)-Na(10)	2.33	O(9)-Na(10)-O(8)	57.65
Na(10)-O(19)	2.33	Na(10)-O(8)-C(7)	88.72
N(12)-C(13)	1.41	C(3)-N(11)-N(12)	114.72
N(11)-N(12)	1.27	C(14)-C(13)-N(12)	115.72
C(7)-O(8)	1.27	C(3)-N(11)-N(12)	114.72
N(11)-C(3)	1.42	C(18)-C(13)-N(12)	125.37
C(7)-O(9)	1.27	N(12)-N(11)-C(3)	114.72
C(16)-C(17)	1.42	C(13)-N(12)-N(11)	115.71

Absorption spectrum and electronic structure of the compound S

Theoretical absorption spectrum of the molecule S optimized in a solvent (water) was calculated using TD B3LYP/6-311+G* method at 250-500 nm by the IEFPCM solvent model. All the DFT

computational calculations were carried out by using the Gaussian 09W package [14]. The equations were solved for 20 excited states, where the computational studies were performed in the presence of water as solvent, using the IEFPCM (integral equation formalism PCM) method coupled to UAKS radii [15]. The TDDFT

method is able to detect the accurate absorption wavelength at a relatively small computing time, which corresponds to the electronic transitions computed on the ground state geometry (Table 7).

Table 7: Electronic absorption spectrum of the compound S calculated by TDB3LYP/6-311+G* method

Excited state	Wavelength (nm)	Excitation energy (eV)	Configurations composition (corresponding transition orbitals)	Oscillator strength (f)
S ₁	475	2.61	0.69(83→85)	0.00
S ₂	388	3.20	0.70(84→85)	1.10
S ₃	351	3.53	0.69 (82→85) + 0.11(82→87)	0.00
S ₄	315	3.94	0.17(77→85) + 0.12 (78→85) - 0.16(79→85) + 0.64(81→85)	0.00
S ₅	310	4.00	0.69(80→85) + 0.10(80→87)	0.00
S ₆	305	4.06	0.56(76→85) - 0.40 (84→86)	0.00
S ₇	356	3.48	0.57(78→85) + 0.41(79→85)	0.00
S ₈	299	4.15	- 0.39(77→85) - 0.29(78→85) + 0.41(79→85) + 0.28(81→85) + 0.10(84→88)	0.00
S ₉	285	4.34	- 0.10(75→85) + 0.51(77→85) - 0.24(78→85) + 0.33(79→85) + 0.17(84→87)	0.09
S ₁₀	278	4.46	0.38(75→85) + 0.38(76→85) + 0.44(84→86)	0.00
S ₁₁	277	4.47	0.68(74→85) + 0.15(83→86)	0.00
S ₁₂	274	4.53	- 0.15(74→85) + 0.68(83→86)	0.00
S ₁₃	271	4.57	0.56(75→85) - 0.16(76→85) - 0.34(84→86) + 0.11(84→87)	0.00
S ₁₄	251	4.95	0.55(78→86) + 0.41(79→86)	0.00
S ₁₅	242	5.12	- 0.13(82→86) + 0.18(82→87) + 0.65(83→87)	0.00
S ₁₆	240	5.17	0.15(77→85) - 0.43(84→87) + 0.49(84→88)	0.00
S ₁₇	239	5.18	- 0.40(82→86) + 0.50(82→87) - 0.22+ 0.11(83→87)	0.00
S ₁₈	236	5.25	0.23(84→87) + 0.21(84→88) + 0.60(84→89)	0.00
S ₁₉	235	5.26	- 0.15(76→86) - 0.11(83→88) + 0.40(84→87) + 0.36(84→88) - 0.36(84→89)	0.00
S ₂₀	234	5.27	0.69(83→88) + 0.11(84→88)	0.00

The experimental absorption spectrum of the dye S (Figure 4b) has a wide absorption at about 350-500 nm which characterized by maximum at 390 nm and calculated spectrum (Figure 4a) shows the oscillation at 388 nm (f = 1.10). The strong peak at 388 nm is due to the Charge-Transfer (CT) excited state. The other peaks are local excited states corresponding to electrons going into anti-bonding orbitals associated with the benzene rings. Excitation of one electron at 388 nm belonged to the transition into the excited singlet state S₂ and describes by a wave function corresponding to one configuration for one-electron excitation (HOMO (84)→LUMO (85)) (Figure 5). Excitation of one electron at 285 nm

and f = 0.09 belonged to the transition into the excited singlet state S₉ and describes by a wave function corresponding to a superposition of five configurations for one-electron excitations (75→85, 77→85, 118→135, 78→85, 79→85 and 84→87). Excitation of an electron from 77 to 85 molecular orbital (MO) gives the main contribution to the formation of the absorption band at 285 nm (Table 7). The other Excitations do not play role in formation of absorption spectrum of the dye S and are forbidden by symmetry. Comparison of calculated and experimental absorption spectra of the compound S demonstrate high accuracy of the constructed model calculations (Figure 4a, b).

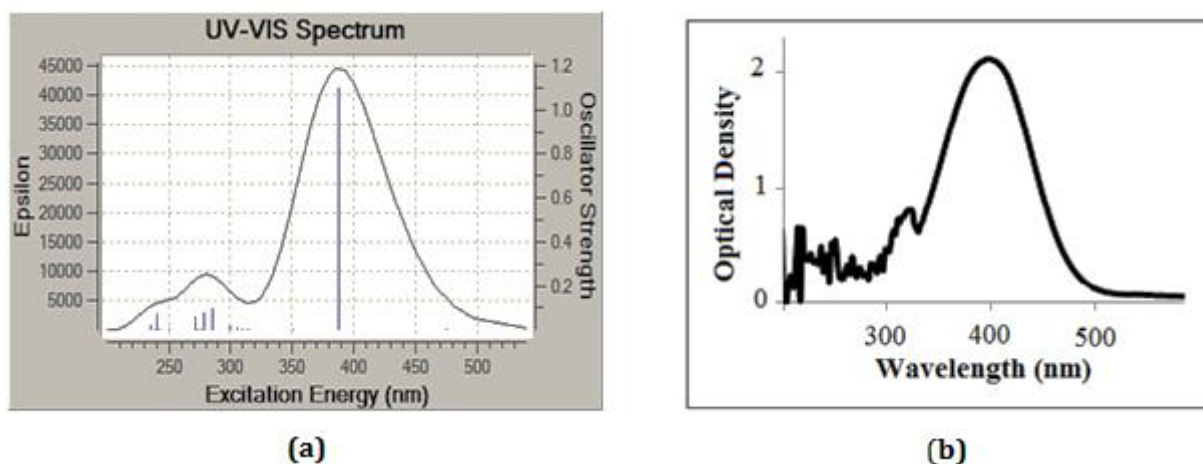


Figure 4: The absorption spectrum of the compound S in Water solution: a) Calculated by TDB3LYP/6-311+G*; b) Experimental at concentration of dye $4.8 \cdot 10^{-4}$ M/l

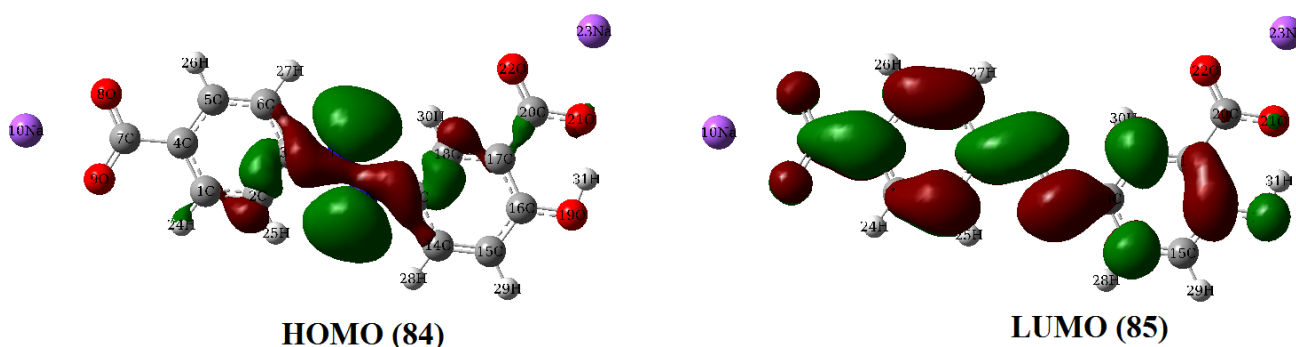


Figure 5: Form of the MO involved in formation of absorption spectrum of the compound S at $\lambda_{\max} = 388$ nm

Conclusions

In the present study, we calculated the geometric parameters, electronic structure, and UV/Vis spectrum of the new synthesized dichroic dye: Sodium (*E*)-5-((4-carboxylatophenyl)diazenyl)-2-hydroxybenzoate (**S**) (trans isomer) by using the B3LYP/6-311+G* method. Based on the quantum-chemical calculations have been synthesized new azo dichroic dye for UV region of spectrum (at $\lambda_{\max} = 388$ nm). At the first time on the basis of polyvinyl alcohol and synthesized compound: Sodium (*E*)-5-((4-carboxylatophenyl)diazenyl)-2-hydroxybenzoate (**S**) thermostable polarizing film absorbing at $\lambda_{\max} = 388$ nm with high polarization efficiency of 97% for optical applications was developed. Stretched colored PVA-films have phenomenon of anisotropy of thermal conductivity. Thermal conductivity in a direction of orientation (λ_{\parallel}) is higher than in a direction perpendicular

orientations (λ_{\perp}). In stretched dyed PVA-films anisotropy of thermal conductivity is observed very clearly (at $R_s = 5.0$, $\lambda_{\parallel} / \lambda_{\perp} = 8.27$).

Disclosure Statement

No potential conflict of interest was reported by the authors.

Funding

This study did not receive any specific grant from funding agencies in the public, commercial, or not-for-profit sectors.

Authors' contributions

All authors contributed toward data analysis, drafting, and revising the paper and agreed to responsible for all the aspects of this work.

Conflict of interest

The authors declare that they have no conflicts of interest in this article.

References

- [1]. Almodarresiyeh H.A., Shahab S.N., Zelenkovsky V.M., Ariko N.G., Filippovich L.N., Agabekov V.E., Calculation of UV, IR, and NMR Spectra of Diethyl 2, 2'-[(1, 1'-Biphenyl)-4, 4'-Diylbis (Azanediyl)] Diacetate. *Journal of Applied Spectroscopy*, **81**:18 [[Google Scholar](#)]
- [2]. Almodarresiyeh H.A., Shahab S.N., Zelenkovsky V.M., Ariko N.G., Filippovich L.N., Agabekov V.E., Calculation of UV, IR, and NMR Spectra of Diethyl 2, 2'-[(1, 1'-Biphenyl)-4, 4'-Diylbis (Azanediyl)] Diacetate. *Journal of Applied Spectroscopy*, 2014, **81**:42 [[Google Scholar](#)]
- [3]. Shahab S., Filippovich L., Kumar R., Darroudi M., Yousefzadeh Borzehandani M., Gomar M., Haji Hajikolaee F., Photochromic properties of the molecule Azure A chloride in polyvinyl alcohol matrix, *Journal of Molecular Structure*, 2015, **1101**:109 [[Crossref](#)], [[Google Scholar](#)], [[Publisher](#)]
- [4]. Shahab S., Filippovich L., Sheikhi M., Kumar R., Dikumar E., Yahyaei H., Muravsky A., Polarization, excited states, trans-cis properties and anisotropy of thermal and electrical conductivity of the 4-(phenyldiazenyl) aniline in PVA matrix, *Journal of Molecular Structure*, 2017, **1141**:703 [[Crossref](#)], [[Google Scholar](#)], [[Publisher](#)]
- [5]. Wang T., Sun H., Lu T., Weerasinghe K.C., Liu D., Hu W., Zhou X., Wang L., Li W., Liu L., Tuning photophysical properties and electronic energy levels of 1-aminoanthraquinone derivatives by introducing N-ethyl substituent, *Journal of Molecular Structure*, 2016, **1116**:256 [[Crossref](#)], [[Google Scholar](#)], [[Publisher](#)]
- [6]. Qiu J., Tang B., Ju B., Xu Y., Zhang S., Stable diazonium salts of weakly basic amines— Convenient reagents for synthesis of disperse azo dyes, *Dyes and Pigments*, 2017, **136**:63 [[Crossref](#)], [[Google Scholar](#)], [[Publisher](#)]
- [7]. a) Shahab S., Almodarresiyeh H.A., Kumar R., Darroudi M., A study of molecular structure, UV, IR, and ¹H NMR spectra of a new dichroic dye on the basis of quinoline derivative, *Journal of Molecular Structure*, 2015, **1088**:105 [[Crossref](#)], [[Google Scholar](#)], [[Publisher](#)] b) Yang Q., Su W., Li S., Li D., Huang Z., Liang F., Transverse magnetic-reflected polarizer for application in surface plasmon resonance configuration. *Optik*, 2017, **133**:32 [[Crossref](#)], [[Google Scholar](#)], [[Publisher](#)]
- [8]. Cisneros-García Z.N., Nieto-Delgado P.G., Rodríguez-Zavala J.G., Conformational analysis on protonation and deprotonation of calmagite in protic solvents and its reactivity through Fukui function, *Dyes and Pigments*, 2015, **121**:188 [[Crossref](#)], [[Google Scholar](#)], [[Publisher](#)]
- [9]. Shahab S., Almodarresiyeh H. A., Filipovich L., Kumar R., Darroudi M., Haji Hajikolaee F., Synthesis of biphenyl derivative and its application as dichroic materials in poly (vinyl alcohol) polarizing films, *Journal of Molecular Structure*, 2016, **1107**:19 [[Crossref](#)], [[Google Scholar](#)], [[Publisher](#)]
- [10]. Shahab S., Kumar R., Darroudi M., Yousefzadeh Borzehandani M., Molecular structure and spectroscopic investigation of sodium (E)-2-hydroxy-5-((4-sulfonatophenyl) diazenyl) benzoate: a DFT study, *Journal of Molecular Structure*, 2015, **1083**:198 [[Crossref](#)], [[Google Scholar](#)], [[Publisher](#)]
- [11]. Shahab S., Sheikhi M., Filippovich L., Dikumar Anatol'evich E., Yahyaei H., Quantum chemical modeling of new derivatives of (E, E)-azomethines: Synthesis, spectroscopic (FT-IR, UV/Vis, polarization) and thermophysical investigations, *Journal of Molecular Structure*, 2017, **1137**:335 [[Crossref](#)], [[Google Scholar](#)], [[Publisher](#)]
- [12]. Shahab S., Filippovich L., Darroudi M., Loiko V.A., Kumar R., Borzehandani M.Y., Molecular structure and UV-Vis spectral analysis of new synthesized azo dyes for application in polarizing films, *Dyes and Pigments*, 2016, **129**:9 [[Crossref](#)], [[Google Scholar](#)], [[Publisher](#)]
- [13]. Shahab S., Filippovich L., Sheikhi M., Yahyaei H., Aharodnikova M., Kumar R., Khaleghian M., Spectroscopic (polarization, excitedstate, FT-IR, UV/Vis and ¹H NMR) and thermophysical investigations of new synthesized azo dye and its application in polarizing film, *American Journal of*

Materials Synthesis and Processing, 2017, 5:17
[[Google Scholar](#)], [[Publisher](#)]
[14]. Frish A., Nielsen A.B., Holder A.J., Gauss view
user manual, Gaussian Inc. Pittsburg, PA. 2001
[[Google Scholar](#)]
[15]. Mennucci B., Cancés E., Tomasi J., Evaluation
of solvent effects in isotropic and anisotropic

dielectrics and in ionic solutions with a unified
integral equation method: theoretical bases,
computational implementation, and numerical
applications, *The Journal of Physical Chemistry B*,
1997, 101:10506 [[Crossref](#)], [[Google Scholar](#)],
[[Publisher](#)]

HOW TO CITE THIS ARTICLE

Siyamak Shahab, Liudmila Filippovich, Masoome Sheikhi. Thermostable Polarizing Film on the Basis of Poly (vinyl alcohol) and New Dichroic Synthesized Azo Dye for Optical Applications: Theoretical and Experimental Investigations. *Chem. Methodol.*, 2023, 7(9) 707-718

DOI: <https://doi.org/10.48309/chemm.2023.53193>

URL: https://www.chemmethod.com/article_53193.html